Acta Crystallographica Section D
Biological Crystallography
ISSN 0907-4449

X-ray structure of *Salmonella typhimurium* uridine phosphorylase complexed with 5-fluorouracil and molecular modelling of the complex of 5-fluorouracil with uridine phosphorylase from *Vibrio cholerae*

Alexander A. Lashkov,[a] Sergey E. Sotnichenko,[a] Igor I. Prokofiev,[a] Azat G. Gabdulkhakov,[a] Igor I. Agapov,[b] Alexander A. Shtil,[c] Christian Betzel,[d] Alexander S. Mironov[e] and Al'bert M. Mikhailov[a]*

[a]A. V. Shubnikov Institute of Crystallography, Russian Academy of Sciences, 59 Leninsky Prospekt, 119333 Moscow, Russian Federation, [b]Shumakov Research Center for Transplantology and Artificial Organs, 1 Shchukinskaya Street, 123182 Moscow, Russian Federation, [c]Blokhin Cancer Center, 24 Kashirskoye Shosse, 115478 Moscow, Russian Federation, [d]University of Hamburg, 85 Notkestrasse, 22603 Hamburg, Germany, and [e]State Research Institute of Genetics and Selection of Industrial Microorganisms, 1 1st Dorozhny Proezd, 117545 Moscow, Russian Federation

Correspondence e-mail: amm@ns.crys.ras.ru

Received 28 December 2011
Accepted 23 April 2012

PDB Reference: *St*UPh–5-fluorouracil, 3nsr.

Uridine phosphorylase (UPh), which is a key enzyme in the reutilization pathway of pyrimidine nucleoside metabolism, is a validated target for the treatment of infectious diseases and cancer. A detailed analysis of the interactions of UPh with the therapeutic ligand 5-fluorouracil (5-FUra) is important for the rational design of pharmacological inhibitors of these enzymes in prokaryotes and eukaryotes. Expanding on the preliminary analysis of the spatial organization of the active centre of UPh from the pathogenic bacterium *Salmonella typhimurium* (*St*UPh) in complex with 5-FUra [Lashkov *et al.* (2009), *Acta Cryst.* F**65**, 601–603], the X-ray structure of the *St*UPh–5-FUra complex was analysed at atomic resolution and an *in silico* model of the complex formed by the drug with UPh from *Vibrio cholerae* (*Vch*UPh) was generated. These results should be considered in the design of selective inhibitors of UPhs from various species.

1. Introduction

Uridine phosphorylase (UPh; EC 2.4.2.3) catalyzes the phosphorylation of pyrimidine nucleotides, which is a vital cellular process (Paege & Schlenk, 1952; Pizzorno *et al.*, 2002). In the presence of phosphate ions, UPh converts uridine to uracil, thereby implementing resynthesis of pyrimidine bases. Furthermore, UPh is the key enzyme in the metabolism of pyrimidine-containing antimicrobial and anticancer drugs (De Clercq, 1980; el Kouni *et al.*, 1988; Jiménez *et al.*, 1989; Paege & Schlenk, 1952). 5-Fluorouracil (5-FUra), a drug that is widely used in the treatment of skin and gastrointestinal malignancies (Pinedo & Peters, 1988; van Groeningen *et al.*, 1992; Visser *et al.*, 1990), exerts its antiproliferative effect by a variety of mechanisms. The drug incorporates into RNA, being recognized as uracil (Pinedo & Peters, 1988). Moreover, 5-FUra is known to inhibit thymidylate synthase and to interfere with DNA replication (Danenberg *et al.*, 1981). Finally, 5-FUra is a substrate of UPh (Pizzorno *et al.*, 2002). General side effects of 5-FUra, including damage to gastric mucosa as well as toxicity to bone marrow, heart muscle and eye tissues (Macdonald, 1999*a*,*b*; Ruiz-Casado *et al.*, 2006), limit the therapeutic use of this drug. However, combination of 5-FUra with specific UPh inhibitors such as 2,2′-anhydrouridine and its derivatives (Iigo *et al.*, 1990) has increased the therapeutic 'window' for 5-FUra and attenuated its side effects (Martin *et al.*, 1989). Synergy of 5-FUra and drugs that block pyrimidine synthesis has been demonstrated to be advantageous for the treatment of infectious diseases and tumours (Jacobs *et al.*, 1979; Michel *et al.*, 1979; Nyhlén *et al.*, 2002).

Table 1
Data-collection and refinement statistics for *St*UPh complexed with 5-FUra.

Values in parentheses are for the highest resolution shell.

Data collection	
Space group	*C*121
Unit-cell parameters (Å, °)	a = 158.26, b = 93.04, c = 149.87, $\alpha = \gamma = 90$, $\beta = 90.65$
No. of molecules per unit cell	6
Molecular weight of hexamer (kDa)	165
No. of amino-acid residues per monomer	253
Wavelength (Å)	0.918
Resolution (Å)	29.3–2.2 (2.25–2.20)
No. of measured reflections	110425 (7124)
No. of unique reflections	99573 (5650)
Completeness (%)	90.2 (79.3)
$R_{\rm merge}$ (%)	0.014 (0.68)
Average $I/\sigma(I)$	12.67 (2.16)
Multiplicity	3.26 (3.24)
Refinement	
Resolution (Å)	10.0–2.2 (2.25–2.20)
Data cutoff	$\sigma(\|F\|) > 0$
No. of $\|F\|$ in working set	103780 (7442)
Completeness of working set (%)	96.9 (98.0)
No. of $\|F\|$ in test set	5149 (141)
$V_{\rm M}$ (Å^3 Da^{-1})	2.27
Solvent content (%)	45.85
No. of protein atoms	16811
No. of water molecules	571
No. of 5-FUra molecules	8
No. of potassium ions	3
$R_{\rm work}$ (%)	20.1
$R_{\rm free}$ (%)	25.8
Average B value for all atoms (Å^2)	38.0
R.m.s. deviations	
Bond lengths (Å)	0.012
Bond angles (°)	1.194
Chirality (Å^3)	0.081
Planarity (Å)	0.003
Error in coordinates from Luzzati plot (Å)	0.333
DPI (Å)	0.233
Estimated maximal error (Å)	0.273
Ramachandran plot†	
Residues in most favoured regions (%)	96.30
Residues in allowed regions (%)	3.11
Residues in outlier regions (%)	0.59

† Obtained using *MolProbity* (Chen *et al.*, 2010).

Focusing on the structural aspects of pharmacological inhibition of UPh, we provided preliminary evidence about the spatial organization of the active centre of UPh from the pathogenic bacterium *Salmonella typhimurium* (*St*UPh) in a ligand-free state and in complexes with therapeutic agents (Lashkov, Zhukhlistova *et al.*, 2009; Lashkov, Zhukhlistova, Sotnichenko *et al.*, 2010). Here, we report the detailed X-ray analysis of the complex formed by 5-FUra with *St*UPh, as well as the molecular docking of 5-FUra into the X-ray structure of uridine phosphorylase from *Vibrio cholerae* (*Vch*UPh).

2. Methods

2.1. Isolation and purification of *St*UPh

The procedures for the isolation and purification of *St*UPh have been described previously (Dontsova *et al.*, 2004; Molchan *et al.*, 1998). Briefly, DNA isolated from *S. typhimurium* was cloned into pBluescript II SK vector (Zolotukhina *et al.*, 2003). *Escherichia coli* strain BL21 (DE3) was propagated on Luria broth solid medium for 12 h at 310 K (Molchan *et al.*, 1998). Protein synthesis was induced with 0.5 m*M* isopropyl β-D-1-thiogalactopyranoside. The protein was purified by chromatography using butyl-Sepharose followed by Q-Sepharose. The activity of the final *St*UPh preparation was 280 U mg^{-1} and its homogeneity was 96% as determined by gel electrophoresis under nondenaturing conditions.

2.2. Crystallization of the *St*UPh–5-FUra complex

The crystals were grown by cocrystallization of *St*UPh with 5-FUra using the hanging-drop vapour-diffusion method (Lashkov, Gabdoulkhakov *et al.*, 2009). The reservoir solution consisted of 160 µl 40%(*m*/*v*) polyethylene glycol 3350, 340 µl 0.1 *M* Tris–maleate–NaOH buffer pH 5.5. The crystallization drop consisted of 2 µl *St*UPh solution (11.3 mg ml^{-1} in 10 m*M* Tris–HCl buffer pH 7.3), 0.3 µl 2-propanol, 2 µl 100 m*M* 5-FUra solution, 2 µl H_2O and 1.3 µl reservoir solution. Crystals (0.07 × 0.3 × 0.5 mm) were obtained after 1–2 weeks and were used for X-ray diffraction analysis.

2.3. Data collection

The X-ray data set was collected by irradiation of *St*UPh–5-FUra crystals under cryogenic conditions (100 K) on beamline 14.2 at BESSY, Berlin, Germany. A CHESS CCD detector was used with an oscillation range $\Delta\varphi$ of 0.5° and a crystal-to-detector distance of 240 mm. The cryoprotectant solution consisted of 100 m*M* Tris–maleate–NaOH buffer pH 5.5, 25%(*w*/*v*) polyethylene glycol 3350, 20%(*v*/*v*) anhydrous glycerol. Data were processed and merged with the *XDS* package (Kabsch, 2001). Statistical parameters of the experimental X-ray data set are presented in Table 1.

2.4. Structure determination and refinement of the *St*UPh–5-FUra complex

The initial phase component of the structure factors for three-dimensional analysis of the *St*UPh–5-FUra complex was obtained by the molecular-replacement method using the program *Phaser* (McCoy *et al.*, 2007). The *B* subunit of *St*UPh in complex with 2,2′-anhydrouridine previously refined to 1.86 Å resolution (Lashkov, Zhukhlistova, Sotnichenko *et al.*, 2010; PDB entry 3fwp) was used as a starting atomic model. The atoms of the ligand and water molecules were removed from the starting model.

The structure of the *St*UPh–5-FUra complex was refined using the *PHENIX* (Adams *et al.*, 2010) and *REFMAC* programs (Murshudov *et al.*, 2011). For refinement of the atomic three-dimensional structure, the simulated-annealing, individual_sites, individual_adp, bulk-solvent modelling and anisotropic scaling options were employed. Refinement using *PHENIX* and *REFMAC* was alternated with manual and semi-automatic applications (*Coot* program; Emsley & Cowtan, 2004; Emsley *et al.*, 2010). Stereochemical limitations, $\sigma_{\rm A}$-weighted electron-density maps with $|F_{\rm obs}| - |F_{\rm calc}|$ and

$2|F_{obs}| - |F_{calc}|$ coefficients and isotropic *B*-factor refinement (ADP) were employed. The positions of water molecules were identified with *Coot* (Emsley & Cowtan, 2004; Emsley *et al.*, 2010) using electron-density maps calculated with $|F_{obs}| - |F_{calc}|$ coefficients. Refinement of coordinates and *B* factors of water molecules was performed using *PHENIX*.

The quality of the final structures was analysed using *PROCHECK* (Laskowski *et al.*, 1993) and the *MolProbity* web service (Chen *et al.*, 2010). The values of statistical parameters of refinement and the quality of refined atomic structures are summarized in Table 1. Figures were drawn using the *PyMOL* program (DeLano, 2002).

2.5. *In silico* modelling of bacterial UPhs

2.5.1. Molecular docking of 5-FUra into the *Vch*UPh X-ray structure. The *AutoDock* 4.2 genetic algorithm was employed for molecular docking of 5-FURa into the uracil-binding site of *Vch*UPh (Morris *et al.*, 2009). The X-ray structure of *Vch*UPh bound to uracil (PDB entry 3pns; Center for Structural Genomics of Infectious Diseases, unpublished work) was used for docking; all molecules of the ligand and the solvent were removed from the *Vch*UPh structure (PDB entry 3pns). The values of the major parameters are presented in Table 2. Default values were used for the parameters not given in the table. The linear dimensions (22.5 × 22.5 × 22.5 Å) of the site of 5-FUra–enzyme interaction corresponded to 60 points along each dimension. The dimensions of the uracil-binding site of the enzyme were 15.1 × 16.4 × 13.6 Å. Several docking solutions were clustered if the r.m.s.d. value of the atomic coordinates of 5-FUra conformers was <1.5 Å (Morris *et al.*, 1998). The optimal solution was selected based on the *AutoDock* scoring function (Morris *et al.*, 2009).

2.5.2. Geometry optimization of the *Vch*UPh–5-FUra complex. Geometry optimization of the complex of *Vch*UPh with 5-FUra was performed with *GROMACS* (Van Der Spoel *et al.*, 2005) using the GROMOS96 force field (Scott *et al.*, 1999). For optimization, we employed energy minimization (EM) and explicit solvent simulations. For the work with the complex of *Vch*UPh with 5-FUra a cubic virtual cell (92.4 Å in each dimension) was used. For *Vch*UPh the distance between the atoms on the surface of the enzyme and the sides of the cell was at least 9 Å. The three-site water model SPC216 (Van Der Spoel *et al.*, 2005) was used for modelling the enzyme structure. The protocol for structural optimization used in this study had been validated by us using the *St*UPh structure (Lashkov, Zhukhlistova, Gabdoulkhakov *et al.*, 2010). The major parameters of the EM protocol are presented in Table 2.

3. Results and discussion

3.1. Primary and quaternary structures

The subunits of the hexameric *St*UPh and *Vch*UPh molecules (Fig. 1) consist of 253 amino-acid residues (Zolotukhina *et al.*, 2003). The primary structures of the subunits of these enzymes are highly homologous to each other as well as to *E. coli* UPh (*Ec*UPh; Zolotukhina *et al.*, 2003). Indeed, the homology between *St*UPh and *Ec*UPh is 97%. Despite this, *St*UPh and *Ec*UPh differ in the efficacy of phosphorolysis of natural nucleosides and their analogues (Molchan *et al.*, 1998). The primary sequence of *Vch*UPh contains 64 substitutions compared with the primary sequence of *Ec*UPh (Zolotukhina *et al.*, 2003). The molecular mass of the subunit of each of the above-mentioned enzymes is 27.5 kDa (Zolotukhina *et al.*, 2003).

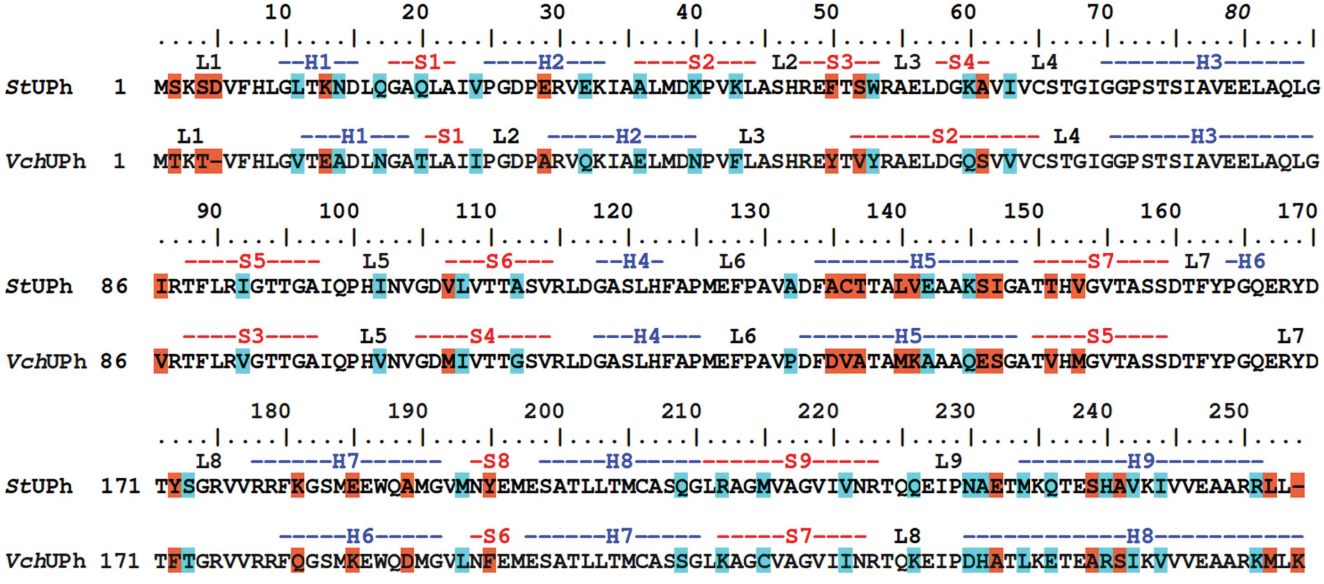

Figure 1
Alignment of the amino-acid sequences of *St*UPh and *Vch*UPh and the secondary structures of the proteins. S, strand; H, helix; L, loop. The alignment was produced using *ClustalW*2 (Larkin *et al.*, 2007). The secondary-structure information was obtained using *PROCHECK* (Laskowski *et al.*, 1993). Nonconserved amino-acid residues are marked in red, similar amino-acid residues are marked in blue and conserved amino-acid residues are not marked.

Table 2
Docking parameters and geometry optimization.

Docking	
No. of GA runs	50
Population size	50
Maximum No. of evaluations	1500000
Step size of quaternion (deg step^{-1})	5.0
Step size of translation (Å step^{-1})	0.2
Step size of torsion (deg step^{-1})	5.0
Geometry optimization	
Coulombtype	PME
dt (ps)	0.002
N_{steps}	500
r_{vdw} (Å)	14
$r_{coulomb}$ (Å)	10
Fourier spacing	0.12

According to the results of protein electrophoresis, the quaternary structures of both *St*UPh and *Vch*UPh are represented by a hexamer comprised of six identical subunits. This composition resembles the structures of *Ec*UPh, *St*UPh and *Vch*UPh (Morgunova *et al.*, 1995; Molchan *et al.*, 1998; Dontsova *et al.*, 2005; PDB entry 3pns). The packing of subunits in the hexamer can be described by the symmetry point group $L_3 3 L_2$. The main structural and functional unit of *St*UPh and *Ec*UPh in the ligand-free state is a homodimer. The hexameric structure of *St*UPh and *Ec*UPh is formed by three homodimers with hydrophobic and hydrogen-bond interactions (Morgunova *et al.*, 1995; Dontsova *et al.*, 2005). The hexameric structure of the *Vch*UPh–5-FUra complex is stabilized by hydrophobic interactions and hydrogen bonds between the amino-acid residues of adjacent homodimers similarly to the *St*UPh–5-FUra complex.

In the *St*UPh–5-FUra complex (PDB entry 3nsr) the subunits within the homodimer interact *via* hydrophobic contacts, ion bridges and hydrogen bonds. These interactions are virtually identical to the respective interactions in ligand-free *St*UPh (Timofeev *et al.*, 2007; Lashkov, Zhukhlistova *et al.*, 2009). The only differences are the Gly26*A* O···Arg48*B* NH2, Asp27*A* N···Arg48*B* NH2, Glu49*A* OE1···Arg48*B* O, His122*A* O···Gln166*B* OE1 and His122*A* O···Gln166*B* NE2 interactions in the *St*UPh–5-FUra complex, which are absent in the ligand-free protein. It is notable that Arg48 involved in the phosphate-binding site is rather mobile.

3.2. Tertiary and secondary structures

The tertiary structure of the subunits of the hexameric *St*UPh and *Vch*UPh molecules is represented by a characteristic trilayer $\alpha/\beta/\alpha$ sandwich architecture (Fig. 2). Comparison of atomic coordinates of the *Vch*UPh–5-FUra complex (using the *SSM* package in *CCP*4; Krissinel & Henrick, 2004; Winn *et al.*, 2011) with the coordinates of the *St*UPh–5-FUra complex obtained by X-ray analysis showed a high homology between the subunits, with an r.m.s.d. value of 0.41 Å. According to calculations using *PROCHECK* (Laskowski *et al.*, 1993), the spatial structure of the subunit of the *St*UPh–5-FUra complex is homologous to that of ligand-free *St*UPh (Lashkov, Zhukhlistova *et al.*, 2009) and consists of helical fragments (38%) and β-strands (27%) (Figs. 1 and 2*a*). The monomer of

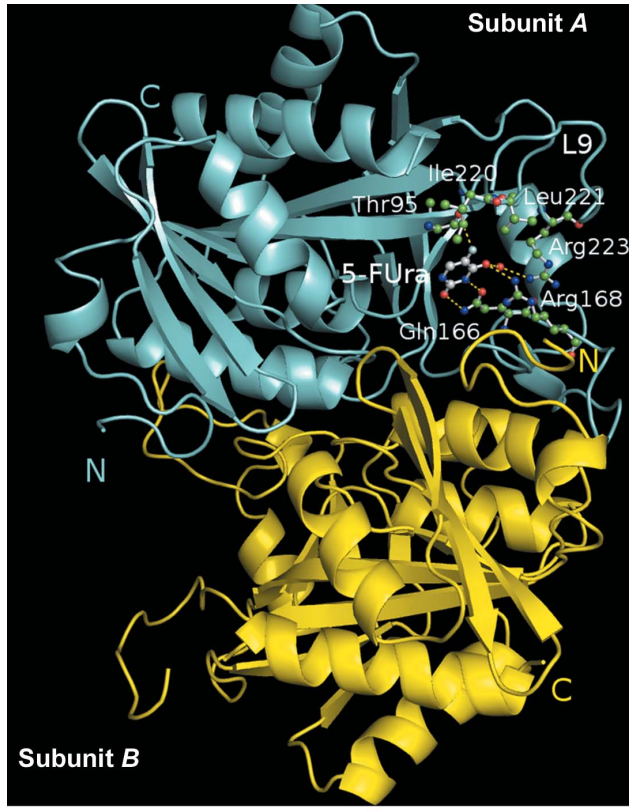

(*a*)

(*b*)

Figure 2
The homodimers of the complexes of 5-FUra with *St*UPh (*a*) and with *Vch*UPh (*b*).

the *Vch*UPh–5-FUra complex consists of 32% helical fragments and 27% β-strands (Figs. 1 and 2*b*).

The conformation of the fragment containing residues 230–233 of L9 in *St*UPh (Fig. 1), as well as the respective fragment in *Ec*UPh, is unstable (Lashkov, Zhukhlistova, Sotnichenko *et al.*, 2010). The helix-to-loop transition, which depends on the presence or absence of the ligand in the catalytic centre, is critical for the enzymatic reaction.

The secondary structure of *Vch*UPh in complex with 5-FUra is in general similar to that of the *St*UPh–5-FUra complex (Figs. 1 and 2). It is worth noting that the functionally important L9 loop in the active centre of *St*UPh contains more amino-acid residues than L8 in *Vch*UPh (Fig. 1). This fact may explain the higher mobility of the L9 gatekeeper in *St*UPh compared with L8 in *Vch*UPh.

3.3. 5-FUra in the active centre of bacterial UPhs

Two active centres have been identified in the homodimers of *St*UPh and of the other bacterial enzymes *Ec*UPh and *Vch*UPh. The catalytic centre of these enzymes possesses sites for binding the phosphate, the uracil and the ribose. The sites for the two latter ligands represent the nucleotide-binding site. The sites for binding the phosphate ion and the nucleoside in the active centre are formed by amino-acid residues from both subunits of the homodimer.

Lashkov, Gabdoulkhakov *et al.* (2009) reported that 5-FUra interacts with the uracil-binding site of the active centre in the *St*UPh–5-FUra complex (PDB entry 3nsr) similarly to drug binding in the *Ec*UPh–5-FUra (Caradoc-Davies *et al.*, 2004) and *h*UPP1–5-FUra (Roosild & Castronovo, 2010) complexes.

The drug–enzyme interactions in the *St*UPh–5-FUra complex are mediated *via* the hydrogen bonds 5-FUra O4 $\cdots$Arg168*A* NH2 (2.9 Å), 5-FUra N3$\cdots$Gln166*A* OE1 (2.8 Å) and 5-FUra O2$\cdots$Gln166*A* NE2 (3.0 Å) (Figs. 2*a*, 3*a* and 3*c*). The O4 atom of 5-FUra interacts with Arg223*A* NH1 *via* water: the distances from the water to 5-FUra O4 and Arg223*A* NH1 are 2.8 and 3.0 Å, respectively. The distance between the F atom in 5-FUra and the carbonyl O atom of Thr95*A* is 3.5 Å; the F atom forms a 3.3 Å contact with the N atom of the main chain of Gly96*A*. Owing to additional bonds with the F atom, the binding of 5-FUra to *St*UPh is stronger than the binding of uracil to *Ec*UPh (Caradoc-Davies *et al.*, 2004) where fluorine is absent. Furthermore, the stacking interaction between the pyrimidine ring of 5-FUra and the aromatic ring of Phe162*A* (the distance between the centres of mass of the aromatic groups of Phe162*A* and 5-FUra is 4.9 Å in *St*UPh) may stabilize the positioning of 5-FUra and other drugs in the active centre of bacterial UPhs (Bu *et al.*, 2005; Caradoc-Davies *et al.*, 2004; Lashkov, Zhukhlistova, Gabdoulkhakov *et al.*, 2010).

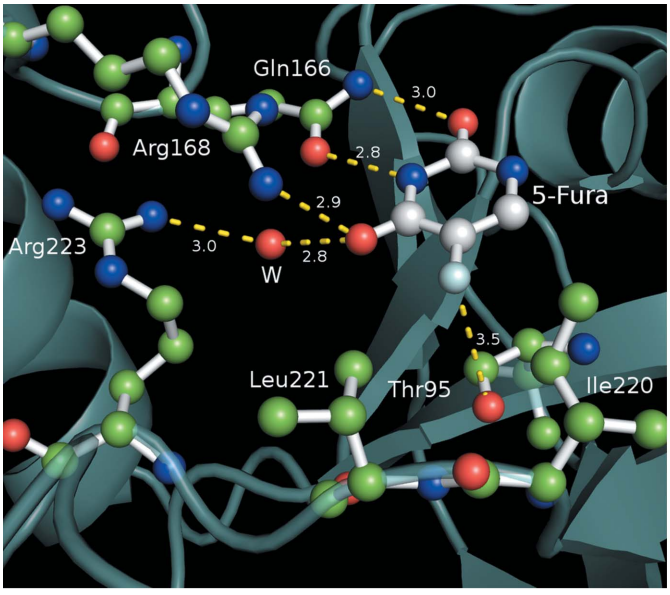

(*a*)

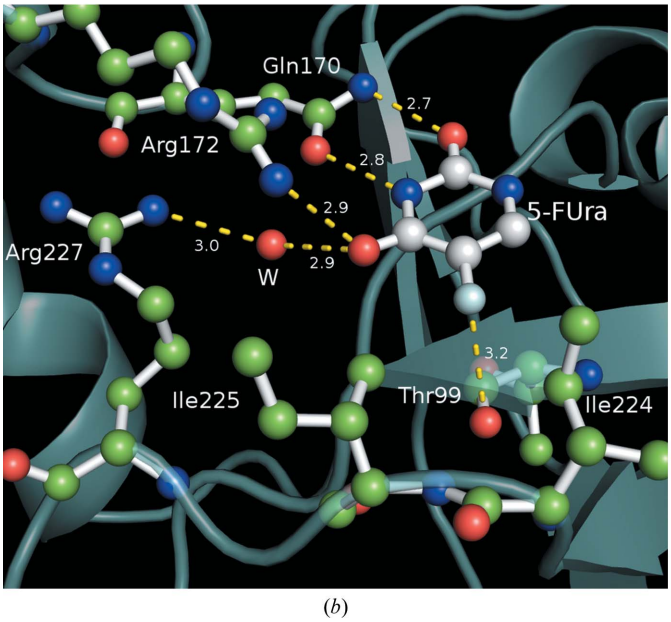

(*b*)

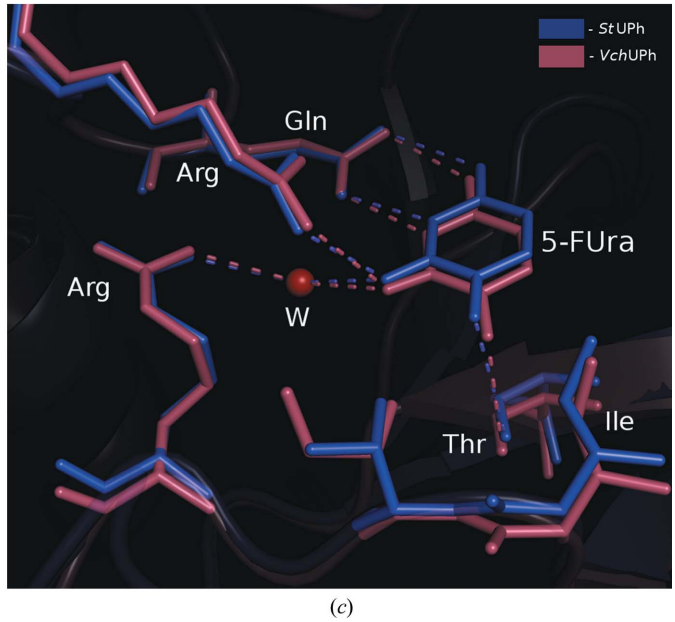

(*c*)

Figure 3
The uracil-binding site in the complexes of 5-FUra with *St*UPh (*a*) and with *Vch*UPh (*b*) and their superposition (*c*).

Comparison of the three-dimensional structures of ligand-free *St*UPh (PDB entry 3dps, subunit *A*) and *St*UPh in complex with 5-FUra (PDB entry 3nsr, subunit *A*) showed that the conformations of Gln166 and Arg168 changed only slightly upon drug binding (the r.m.s.d.s for the main chains were 0.54 and 0.69 Å, respectively, and those for the side chains were 0.88 and 0.65 Å, respectively). In contrast, the conformation of Arg223 changed substantially (the r.m.s.d.s for the side chain and the main chain were 1.37 and 1.76 Å, respectively). It may be hypothesized that Arg223 plays an important role in the conformational transitions of the L9 loop that are important for enzymatic function. Similar conformational changes of Arg223 have been detected in the complex of *St*UPh with its inhibitor 2,2′-anhydrouridine (Lashkov, Zhukhlistova, Sotnichenko *et al.*, 2010), whereas in the *h*UPP1–5-FUra complex (Roosild *et al.*, 2009; Roosild & Castronovo, 2010) the conformation of Arg275 (Arg223 in *St*UPh) remained unchanged.

Molecular docking of 5-FUra into the binding site of the *Vch*UPh X-ray structure revealed the following hydrogen bonds (Figs. 3*b* and 3*c*): 5-FUra O4···Arg 172*A* NH2 (2.9 Å), 5-FUra N3···Gln170A OE1 (2.8 Å) and 5-FUra O2···Gln170*A* NE2 (2.7 Å). A van der Waals interaction (3.2 Å) was established between 5-FUra F and the carboxy group of Thr99*A*. The 5-FUra O4 atom interacted with Arg227, the analogue of Arg223 in *St*UPh, *via* a water molecule: the distances from the water to 5-FUra O4 and Arg227*A* NE are 2.7 and 2.9 Å, respectively.

The hydrophobic environment of the pyrimidine ring in 5-FUra is formed by the following residues: Ile220 and Val221 in *St*UPh, Leu272, Leu273 and Ile281 in *h*UPP1 (Roosild *et al.*, 2009; Roosild & Castronovo, 2010) and Ile224 and Val225 in *Vch*UPh.

In the *h*UPP1–5-FUra complex (Roosild & Castronovo, 2010) the drug is located in the uracil-binding site similarly as in the *St*UPh–5-FUra complex. The hydrogen bonds between *h*UPP1 and 5-FUra are formed by Gln217 and Arg219; the Arg275–drug interaction is mediated by a water molecule. Roosild and Castronovo found an interaction of the carbonyl group of the main chain of Ser142 (Thr95 in *St*UPh) with 5-FUra (Roosild & Castronovo, 2010). Given that the conformation of the 5-FUra-binding site in *h*UPP1 (Gln217, Arg219 and Arg275) is similar to the conformation of the respective sites in *St*UPh and *Ec*UPh (Gln166, Arg168 and Arg223) and *Vch*UPh (Gln170, Arg172 and Arg227), the uracil-binding sites in the active centres of all studied enzymes are conserved. Most probably, the mechanism of interaction with the drug is the same for each UPh, at least from the viewpoint of its three-dimensional organization.

4. Conclusion

The structures of the complexes formed by 5-FUra with the active centres of *St*UPh, *Vch*UPh, *Ec*UPh and *h*UPP1 (Bu *et al.*, 2005; Roosild & Castronovo, 2010) are similar (Fig. 3*c*). The binding of 5-FUra to each studied enzyme differs from the binding of the nonfluorinated pyrimidine bases uracil or thymidine (Bu *et al.*, 2005; Caradoc-Davies *et al.*, 2004) by the formation of contacts between the F atom and the carbonyl O atom in Thr95 and the N atom in the main chain of Gly96.

Binding of 5-FUra into the active centre of *St*UPh changes the conformation of Arg223, a residue that interacts with the drug *via* a water molecule. A similar shift of the Arg223 conformation occurs upon the binding of 5-FUra to *Ec*UPh (Caradoc-Davies *et al.*, 2004). In turn, conformational changes of this residue are associated with conformational transitions of the functionally important L9 loop in *St*UPh. In *h*UPP1 (Roosild & Castronovo, 2010; Roosild *et al.*, 2009) the conformation of Arg275 (the analogue of Arg223 in *St*UPh) remains unaltered upon binding of 5-FUra or other ligands.

Thus, Arg223 should be considered as a residue that is critical for catalysis in the bacterial enzymes *St*UPh and *Ec*UPh.

This study was supported by the A. V. Shubnikov Institute of Crystallography, Russian Academy of Sciences and by a grant from the Ministry of Education and Science of the Russian Federation (contract No. 16.512.11.2235).

References

Adams, P. D. *et al.* (2010). *Acta Cryst.* D**66**, 213–221.
Bu, W., Settembre, E. C., el Kouni, M. H. & Ealick, S. E. (2005). *Acta Cryst.* D**61**, 863–872.
Caradoc-Davies, T. T., Cutfield, S. M., Lamont, I. L. & Cutfield, J. F. (2004). *J. Mol. Biol.* **337**, 337–354.
Chen, V. B., Arendall, W. B., Headd, J. J., Keedy, D. A., Immormino, R. M., Kapral, G. J., Murray, L. W., Richardson, J. S. & Richardson, D. C. (2010). *Acta Cryst.* D**66**, 12–21.
Danenberg, P. V., Heidelberger, C., Mulkins, M. A. & Peterson, A. R. (1981). *Biochem. Biophys. Res. Commun.* **102**, 654–658.
De Clercq, E. (1980). *Methods Find. Exp. Clin. Pharmacol.* **2**, 253–267.
DeLano, W. L. (2002). *PyMOL*. http://www.pymol.org.
Dontsova, M. V., Gabdoulkhakov, A. G., Molchan, O. K., Lashkov, A. A., Garber, M. B., Mironov, A. S., Zhukhlistova, N. E., Morgunova, E. Y., Voelter, W., Betzel, C., Zhang, Y., Ealick, S. E. & Mikhailov, A. M. (2005). *Acta Cryst.* F**61**, 337–340.
Dontsova, M. V., Savochkina, Y. A., Gabdoulkhakov, A. G., Baidakov, S. N., Lyashenko, A. V., Zolotukhina, M., Errais Lopes, L., Garber, M. B., Morgunova, E. Y., Nikonov, S. V., Mironov, A. S., Ealick, S. E. & Mikhailov, A. M. (2004). *Acta Cryst.* D**60**, 709–711.
Emsley, P. & Cowtan, K. (2004). *Acta Cryst.* D**60**, 2126–2132.
Emsley, P., Lohkamp, B., Scott, W. G. & Cowtan, K. (2010). *Acta Cryst.* D**66**, 486–501.
Groeningen, C. J. van, Peters, G. J. & Pinedo, H. M. (1992). *Semin. Oncol.* **19**, 148–154.
Iigo, M., Nishikata, K., Nakajima, Y., Szinai, I., Veres, Z., Szabolcs, A. & De Clercq, E. (1990). *Biochem. Pharmacol.* **39**, 1247–1253.
Jacobs, J. Y., Michel, J. & Sacks, T. (1979). *Antimicrob. Agents Chemother.* **15**, 580–586.
Jiménez, B. M., Kranz, P., Lee, C. S., Gero, A. M. & O'Sullivan, W. J. (1989). *Biochem. Pharmacol.* **38**, 3785–3789.
Kabsch, W. (2001). *International Tables for Crystallography*, Vol. *F*, edited by M. G. Rossmann & E. Arnold: Dordrecht: Kluwer Academic Publishers.
el Kouni, M. H., Naguib, F. N., Niedzwicki, J. G., Iltzsch, M. H. & Cha, S. (1988). *J. Biol. Chem.* **263**, 6081–6086.
Krissinel, E. & Henrick, K. (2004). *Acta Cryst.* D**60**, 2256–2268.

Larkin, M. A., Blackshields, G., Brown, N. P., Chenna, R., McGettigan, P. A., McWilliam, H., Valentin, F., Wallace, I. M., Wilm, A., Lopez, R., Thompson, J. D., Gibson, T. J. & Higgins, D. G. (2007). *Bioinformatics*, **23**, 2947–2948.
Lashkov, A. A., Gabdoulkhakov, A. G., Shtil, A. A. & Mikhailov, A. M. (2009). *Acta Cryst.* F**65**, 601–603.
Lashkov, A. A., Zhukhlistova, N. E., Gabdoulkhakov, A. H., Shtil, A. A., Efremov, R. G., Betzel, C. & Mikhailov, A. M. (2010). *Acta Cryst.* D**66**, 51–60.
Lashkov, A. A., Zhukhlistova, N. E., Gabdulkhakov, A. G. & Mikhailov, A. M. (2009). *Crystallogr. Rep.* **54**, 267–278.
Lashkov, A., Zhukhlistova, N., Sotnichenko, S., Gabdulkhakov, A. & Mikhailov, A. M. (2010). *Crystallogr. Rep.* **55**, 41–57.
Laskowski, R. A., MacArthur, M. W., Moss, D. S. & Thornton, J. M. (1993). *J. Appl. Cryst.* **26**, 283–291.
Macdonald, J. S. (1999*a*). *Am. J. Clin. Oncol.* **22**, 475–480.
Macdonald, J. S. (1999*b*). *Oncology (Williston Park)*, **13**, 33–34.
Martin, D. S., Stolfi, R. L. & Sawyer, R. C. (1989). *Cancer Chemother. Pharmacol.* **24**, 9–14.
McCoy, A. J., Grosse-Kunstleve, R. W., Adams, P. D., Winn, M. D., Storoni, L. C. & Read, R. J. (2007). *J. Appl. Cryst.* **40**, 658–674.
Michel, J., Jacobs, J. Y. & Sacks, T. (1979). *Antimicrob. Agents Chemother.* **16**, 761–766.
Molchan, O. K., Dmitrieva, N. A., Romanova, D. V., Lopes, L. E., Debabov, V. G. & Mironov, A. S. (1998). *Biochemistry*, **63**, 195–199.
Morgunova, E. Y., Mikhailov, A. M., Popov, A. N., Blagova, E. V., Smirnova, E. A., Vainshtein, B. K., Mao, C., Armstrong, S. R., Ealick, S. E., Komissarov, A. A., Linkova, E. V., Burlakova, A. A., Mironov, A. S. & Debabov, V. G. (1995). *FEBS Lett.* **367**, 183–187.
Morris, G. M., Goodsell, D. S., Halliday, R. S., Huey, R., Hart, W. E., Belew, R. K. & Olson, A. J. (1998). *J. Comput. Chem.* **19**, 1539–1662.
Morris, G. M., Huey, R., Lindstrom, W., Sanner, M. F., Belew, R. K., Goodsell, D. S. & Olson, A. J. (2009). *J. Comput. Chem.* **30**, 2785–2791.
Murshudov, G. N., Skubák, P., Lebedev, A. A., Pannu, N. S., Steiner, R. A., Nicholls, R. A., Winn, M. D., Long, F. & Vagin, A. A. (2011). *Acta Cryst.* D**67**, 355–367.
Nyhlén, A., Ljungberg, B., Nilsson-Ehle, I. & Odenholt, I. (2002). *Chemotherapy*, **48**, 71–77.
Paege, L. M. & Schlenk, F. (1952). *Arch. Biochem. Biophys.* **40**, 42–49.
Pinedo, H. M. & Peters, G. F. (1988). *J. Clin. Oncol.* **6**, 1653–1664.
Pizzorno, G., Cao, D., Leffert, J. J., Russell, R. L., Zhang, D. & Handschumacher, R. E. (2002). *Biochim. Biophys. Acta*, **1587**, 133–144.
Roosild, T. P. & Castronovo, S. (2010). *PLoS One*, **5**, e12741.
Roosild, T. P., Castronovo, S., Fabbiani, M. & Pizzorno, G. (2009). *BMC Struct. Biol.* **9**, 14.
Ruiz-Casado, A., García, M. D. & Racionero, M. A. (2006). *Clin. Transl. Oncol.* **8**, 624.
Scott, W. R. P., Hünenberger, P. H., Tironi, I. G., Mark, A. E., Billeter, S. R., Fennen, J., Torda, A. E., Huber, T., Krüger, P. & van Gunsteren, W. F. (1999). *J. Phys. Chem. A*, **103**, 3596–3607.
Timofeev, V. I., Pavlyuk, B. F., Lashkov, A. A., Seregina, T. A., Gabdulkhakov, A. G., Vainshtein, B. K. & Mikhailov, A. M. (2007). *Crystallogr. Rep.* **52**, 1072–1078.
Van Der Spoel, D., Lindahl, E., Hess, B., Groenhof, G., Mark, A. E. & Berendsen, H. J. (2005). *J. Comput. Chem.* **26**, 1701–1718.
Visser, G. W., Gorree, G. C., Peters, G. J. & Herscheid, J. D. (1990). *Cancer Chemother. Pharmacol.* **26**, 205–209.
Winn, M. D. *et al.* (2011). *Acta Cryst.* D**67**, 235–242.
Zolotukhina, M., Ovcharova, I., Eremina, S., Errais Lopes, L. & Mironov, A. S. (2003). *Res. Microbiol.* **154**, 510–520.